Computational and Applied Mathematics (2024) 43:307
https://doi.org/10.1007/s40314-024-02837-w

Robust and accurate reconstruction of the time-dependent continuous volatility from option prices

Youngjin Hwang[1] · Taehee Lee[2] · Soobin Kwak[1] · Seungyoon Kang[1] · Seokjun Ham[1] · Junseok Kim[1]

Received: 27 February 2024 / Revised: 9 May 2024 / Accepted: 21 June 2024 /
Published online: 1 July 2024

Abstract
In this paper, we propose a robust and accurate reconstruction algorithm for the time-dependent continuous volatility function using observed option prices from the financial market and the Black–Scholes (BS) equation. The proposed algorithm consists of two steps: First, a time-dependent piecewise-constant volatility function is calculated. Second, a continuous volatility function is reconstructed by continuously connecting the jumps of the piecewise-constant volatility values at the expiration dates. We validate the accuracy and robustness of the proposed reconstruction of time-dependent continuous volatility by employing manufactured volatility and real financial market price data.

Keywords Continuous volatility · Black–Scholes equation · Finite difference method

1 Introduction

The Black–Scholes (BS) partial differential equation (PDE) is one of the most widely used models in the field of option pricing (Black and Scholes 1973). The main objective of this paper is to develop a numerical algorithm that reconstructs time-dependent continuous volatil-

✉ Junseok Kim
cfdkim@korea.ac.kr

Youngjin Hwang
youngjin_hwang@korea.ac.kr

Taehee Lee
lth0407@korea.ac.kr

Soobin Kwak
soobin23@korea.ac.kr

Seungyoon Kang
heroe2401@korea.ac.kr

Seokjun Ham
seokjun@korea.ac.kr

1 Department of Mathematics, Korea University, Seoul, State 02841, Republic of Korea

2 Program in Actuarial Science and Financial Engineering, Korea University, Seoul, State 02841, Republic of Korea

ity using the BS PDE. In a previous work (Rodrigo and Mamon 2006), the authors explored a transformation of the equation involving time-varying parameters, aiming for a more comprehensive approach. The focus lies on incorporating observed market option prices across various strike prices and expiration dates:

$$\frac{\partial u(S,t)}{\partial t} + \frac{1}{2}[\sigma(t)S]^2 \frac{\partial^2 u(S,t)}{\partial S^2} + rS\frac{\partial u(S,t)}{\partial S} - ru(S,t) = 0, \tag{1}$$

for $(S, t) \in \mathbb{R}^+ \times [0, T)$, where $u(S, t)$ is the option value of the underlying price S at time t. Here, $\sigma(t)$ is the time-dependent volatility function of time t. The final condition is the payoff function $u(S, T) = \Lambda(S)$ at expiry T.

To resolve issues related to a constant volatility model, diverse methods have been proposed, including local volatility (Itkin and Lipton 2018) and stochastic local volatility models (Wyns and In't Hout 2018; Zhang et al. 2022; Yoon et al. 2022; Kim et al. 2023). Kim et al. (2021) developed a numerical algorithm for the reconstruction of the local volatility function. When the price evolution of a financial asset consists of known prices of European options on that asset, local volatility models show a good performance (Gatheral et al. 2012). In order to extend the financial theory to the fractional structure of the financial market, a large number of studies dedicated to the fractional BS equation were introduced. Iqbal and Wei (2021) studied the time fractional BS equation with a double barriers option based on the time-dependent volatility coefficient. The L_1-FDIA scheme, Tikhonov regularization, and Legendre-collocation method are used to numerically solve the governing equation. Tikhonov regularization is an important tool for the inverse problem in mathematical finance. Crépey (2003) applied Tikhonov regularization for calibration of the local volatility function in a generalized BS equation. Park et al. (2022) presented a calibration algorithm of volatility and interest rate functions. Based on the fractional Vasicek interest rate model, Zhao and Xu (2022) proposed the calibration of the time-dependent volatility function. They applied an implicit finite difference method (FDM) and dealt with European options. In (Georgiev and Vulkov 2019), the authors presented the numerical approximation of the implied volatility for European options under jump-diffusion models. Georgiev and Vulkov (2020) proposed a robust algorithm for the time-dependent volatility function. They observed one- and two-asset BS equations and used special decomposition for the algorithm. Furthermore, Georgiev and Vulkov (2021) also proposed a fast and robust numerical scheme to reconstruct the time-dependent volatility function. They considered a predictor–corrector method to handle the non-uniqueness of the volatility function minimizer. Jin et al. (2018) studied a BS model under a time-dependent volatility function using a fully implicit FDM. A cost function is defined and the steepest descent method is applied to minimize the cost function. Numerical results using financial market data are presented to demonstrate the performance of the proposed method. Schied and Stadje (2007) studied a delta hedging strategy from a local volatility model. The robustness of the proposed method holds for a standard BS equation when a path-dependent derivative is hedged with a convex payoff function. They proved that the robustness also holds for other local volatility models when the payoff function is directionally convex.

This article follows the following organization. Section 2 provides a detailed numerical algorithm of the proposed method. The computer tests are presented in Sect. 3. Finally, Sect. 4 presents the conclusions drawn from the study.

2 Numerical algorithm

In this section, we introduce the proposed numerical algorithm. Let $\tau = T - t$. Then, Eq. (1) can be expressed as

$$\frac{\partial u(S,\tau)}{\partial \tau} = \frac{1}{2}[\sigma(\tau)S]^2 \frac{\partial^2 u(S,\tau)}{\partial S^2} + rS\frac{\partial u(S,\tau)}{\partial S} - ru(S,\tau), \quad (S,t) \in \Omega \times (0,T]. \quad (2)$$

We solve Eq. (2) using a finite difference method (Jeong et al. 2016). We define the non-uniform asset price domain $\Omega = \{S_1,\ S_2,\ \ldots, S_{N_S}\}$, where N_S is the number of spatial steps. The non-uniform spatial step size is defined as $h_i = S_{i+1} - S_i$ for $i =, 1, 2, \ldots, N_S$. Furthermore, we consider the zero Dirichlet boundary condition at $S = 0$ and the linear boundary condition at $S = L$ (Windcliff et al. 2004). Thus, an external artificial node S_{N_s+1} is required to satisfy the boundary conditions at $S = L$. Figure 1 shows a schematic of the non-uniform asset price domain with an external artificial node S_{N_x+1}. Note that there is a method which does not use the far-field boundary condition (Lee et al. 2023). Let u_i^n be the numerical approximation of $u(S_i, n\Delta\tau)$ for $i = 1,\ 2, \ldots,\ N_S$ and $n = 0,\ 1, \ldots,\ N_\tau$, where $\Delta\tau = T/N_\tau$ N_τ is the number of temporal steps (Fig. 2).

Let σ^n be the discrete variable volatility $\sigma(n\Delta\tau)$. We discretize Eq. (2) using the non-uniform finite difference scheme in space and a fully implicit scheme in time.

$$\frac{u_i^{n+1} - u_i^n}{\Delta\tau} = \frac{(\sigma^{n+1}S_i)^2}{2}\left(\frac{\partial^2 u}{\partial S^2}\right)_i^{n+1} + rS_i\left(\frac{\partial u}{\partial S}\right)_i^{n+1} - ru_i^{n+1}, \quad (3)$$

where

$$\left(\frac{\partial^2 u}{\partial S^2}\right)_i^{n+1} = \frac{2u_{i-1}^{n+1}}{h_{i-1}(h_{i-1}+h_i)} - \frac{2u_i^{n+1}}{h_{i-1}h_i} + \frac{2u_{i+1}^{n+1}}{h_i(h_{i-1}+h_i)}, \quad (4)$$

$$\left(\frac{\partial u}{\partial S}\right)_i^{n+1} = \frac{-h_i u_{i-1}^{n+1}}{h_{i-1}(h_{i-1}+h_i)} + \frac{(h_i - h_{i-1})u_i^{n+1}}{h_{i-1}h_i} + \frac{h_{i-1}u_{i+1}^{n+1}}{h_i(h_{i-1}+h_i)}. \quad (5)$$

Then, we can rewrite the above Eq. (3) as

$$\alpha_i u_{i-1}^{n+1} + \beta_i u_i^{n+1} + \gamma_i u_{i+1}^{n+1} = b_i, \quad \text{for } i = 2, \ldots, N_S, \quad (6)$$

where

$$\alpha_i = \frac{rS_ih_i}{h_{i-1}(h_{i-1}+h_i)} - \frac{(\sigma^{n+1}S_i)^2}{h_{i-1}(h_{i-1}+h_i)},$$

$$\beta_i = \frac{1}{\Delta\tau} - \frac{rS_i(h_i - h_{i-1})}{h_{i-1}h_i} + \frac{(\sigma^{n+1}S_i)^2}{h_{i-1}h_i} + r,$$

$$\gamma_i = -\frac{S_ih_{i-1}}{h_i(h_{i-1}+h_i)} - \frac{(\sigma^{n+1}S_i)^2}{h_i(h_{i-1}+h_i)}, \text{ and } b_i = \frac{u_i^n}{\Delta\tau}.$$

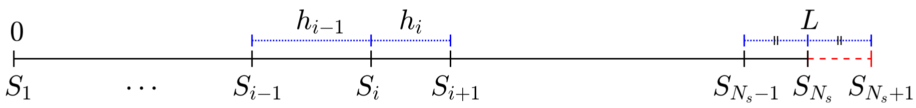

Fig. 1 Schematic of the non-uniform grid with external artificial node S_{N_x+1}

We apply the zero Dirichlet condition at $S = 0$ and the linear condition at $S = L$.

$$u(0,\tau) = 0,\ \frac{\partial^2 u(L,\tau)}{\partial S^2} = 0.$$

Thus,

$$u_1^{n+1} = 0,\ u_{N_S+1}^{n+1} = 2u_{N_S}^{n+1} - u_{N_S-1}^{n+1}.$$

By substituting the relation and $u_{N_S+1}^{n+1} = 2u_{N_S}^{n+1} - u_{N_S-1}^{n+1}$ into Eq. (6), we get

$$(\alpha_{N_S} - \gamma_{N_S})u_{N_S-1}^{n+1} + (\beta_{N_S} + 2\gamma_{N_S})u_{N_S}^{n+1} = b_{N_S}^n. \tag{7}$$

The matrix form of the linear system (6) and (7) can be rewritten as

$$\begin{pmatrix} \beta_2 & \gamma_2 & 0 & \cdots & 0 \\ \alpha_3 & \beta_3 & \gamma_3 & \cdots & 0 \\ \vdots & \ddots & \ddots & \ddots & \vdots \\ 0 & \ldots\ \alpha_{N_x-1} & \beta_{N_x-1} & & \gamma_{N_x-1} \\ 0 & \ldots\ 0 & \alpha_{N_x} - \gamma_{N_x} & & \beta_{N_x} + 2\gamma_{N_x} \end{pmatrix} \begin{pmatrix} u_2^{n+1} \\ u_3^{n+1} \\ \vdots \\ u_{N_x-1}^{n+1} \\ u_{N_x}^{n+1} \end{pmatrix} = \begin{pmatrix} b_2^n \\ b_3^n \\ \vdots \\ b_{N_x-1}^n \\ b_{N_x}^n \end{pmatrix}, \tag{8}$$

where we have used $u_1^{n+1} = 0$. We apply the Thomas algorithm (Ames 2014) to solve the discrete tri-diagonal system (8).

Following this, we present the numerical algorithm to reconstruct the time-dependent volatility function using option prices. Let U_β^α be the market option prices with the expiration date T_α for $\alpha = 1, \cdots, M_t$ and the exercise price K_β for $\beta = 1, \cdots, M_k$. For $\alpha = 1, \ldots, M_t$, we determine a piecewise-constant volatility function $\sigma(t)$ using the given price data in the least-squares sense:

$$\mathcal{E}(\sigma) = \frac{1}{M_k} \sum_{\beta=1}^{M_k} [u_{K_\beta}(\sigma, S_0, T_\alpha) - U_\beta^\alpha]^2, \tag{9}$$

where $u_{K_\beta}(\sigma, S_0, T_\alpha)$ represents the numerical solution at $S = S_0$ of Eq (2) with the strike price K_β at time T_α. Let the piecewise volatility constants be denoted as $\boldsymbol{\sigma} = (\sigma_1, \ldots, \sigma_\alpha)$. We define a piecewise-constant volatility function $V_{\boldsymbol{\sigma}}$ as

$$V_{\boldsymbol{\sigma}}(t) = \sigma_v,\ \text{if } T_{v-1} < t \le T_v,\ 1 \le v \le \alpha.$$

First, we apply the steepest descent method to calculate a piecewise constant volatility σ_α that minimizes the cost function $\mathcal{E}(V_{\boldsymbol{\sigma}})$ for $\alpha = 1, \ldots, M_t$. We define the tol as the tolerance for the cost function in the steepest descent method. The details of the overall steps are given in Algorithm 1.

Next, we consider the following modified BS formula, which works for any integrable deterministic volatility function (Jiang and Li 2005).

$$u(S,\tau) = SN(d_1) - Ke^{-r\tau}N(d_2), \tag{10}$$

where

$$d_1 = \frac{\ln\frac{S}{K} + r\tau + \int_0^\tau \sigma^2(t)dt}{\sqrt{\int_0^\tau \sigma^2(t)dt}},\ d_2 = \frac{\ln\frac{S}{K} + r\tau - \int_0^\tau \sigma^2(t)dt}{\sqrt{\int_0^\tau \sigma^2(t)dt}} = d_1 - \sqrt{\int_0^\tau \sigma^2(t)dt}.$$

Algorithm 1 Piecewise-constant volatility function using the steepest descent method

INPUT tolerance tol; maximum number of iterations N; initial approximation σ_1.
OUTPUT approximation solution $\boldsymbol{\sigma} = (\sigma_1, \ldots, \sigma_{M_t})$.
Step 1 For $v = 1, \ldots, M_t$ do Steps 2–12.
  Step 2 If $v \geq 2$ then
    set $\sigma_v = \sigma_{v-1}$.
  Step 3 Set $\boldsymbol{\sigma} = (\sigma_1, \ldots, \sigma_v)$;
    $error = 2tol$.
    $k = 1$.
  Step 4 While ($k \leq N$ and $error \geq tol$) do Steps 5–11.
    Step 5 Set $g = 1$; $a_1 = -g$; $a_2 = 0$; $a_3 = g$;
      $\mathcal{E}_2 = \mathcal{E}(V_{\boldsymbol{\sigma}}(t))$;
      $\boldsymbol{\sigma}' = (\sigma_1, \ldots, \sigma_v + a_1)$; $\mathcal{E}_1 = \mathcal{E}(V_{\boldsymbol{\sigma}'}(t))$;
      $\boldsymbol{\sigma}' = (\sigma_1, \ldots, \sigma_v + a_3)$; $\mathcal{E}_3 = \mathcal{E}(V_{\boldsymbol{\sigma}'}(t))$.
      $h_1 = (\mathcal{E}_1 + \mathcal{E}_3 - 2\mathcal{E}_2)/g^2$; $h_2 = (\mathcal{E}_3 - \mathcal{E}_1)/g$;
      $a_0 = -0.5h_2/h_1$;
      $\boldsymbol{\sigma}' = (\sigma_1, \ldots, \sigma_v + a_0)$; $\mathcal{E}_0 = \mathcal{E}(V_{\boldsymbol{\sigma}'}(t))$.
    Step 6 While $\Big((\mathcal{E}_3 \geq \mathcal{E}_2$ and $\mathcal{E}_1 \geq \mathcal{E}_2)$ or $(\mathcal{E}_2 \geq \mathcal{E}_3$ and $\mathcal{E}_2 \geq \mathcal{E}_1)$ or $\sigma_v + a_1 < 0\Big)$
      do Steps 7 and 8.
      Step 7 Set $g = g/2$; $a_1 = -g$; $a_3 = g$;
        $\boldsymbol{\sigma}' = (\sigma_1, \ldots, \sigma_v + a_1)$; $\mathcal{E}_1 = \mathcal{E}(V_{\boldsymbol{\sigma}'}(t))$;
        $\boldsymbol{\sigma}' = (\sigma_1, \ldots, \sigma_v + a_3)$; $\mathcal{E}_3 = \mathcal{E}(V_{\boldsymbol{\sigma}'}(t))$.
      Step 8 If $g < tol/2$ then
        OUTPUT ('No likely improvement');
        OUTPUT $\boldsymbol{\sigma} = (\sigma_1, \ldots, \sigma_v)$.
        STOP.
    Step 9 Set $h_1 = (\mathcal{E}_3 + \mathcal{E}_1 - 2\mathcal{E}_2)/g^2$; $h_2 = (\mathcal{E}_3 - \mathcal{E}_1)/g$;
      $a_0 = -0.5h_2/h_1$;
      $\boldsymbol{\sigma}' = (\sigma_1, \ldots, \sigma_v + a_0)$; $\mathcal{E}_0 = \mathcal{E}(V_{\boldsymbol{\sigma}'}(t))$.
    Step 10 Find a from $\{a_0, a_1, a_3\}$ so that $\mathcal{E} = \mathcal{E}(V_{\boldsymbol{\sigma}'}(t)) = \min\{\mathcal{E}_0, \mathcal{E}_1, \mathcal{E}_3\}$,
      where $\boldsymbol{\sigma}' = (\sigma_1, \ldots, \sigma_v + a)$.
    Step 11 Set $\boldsymbol{\sigma} = (\sigma_1, \ldots, \sigma_v + a)$;
      $k = k + 1$;
      $error = |\mathcal{E} - \mathcal{E}_2|$.
  Step 12 If $k = N + 1$ then
    OUTPUT ('Maximum iterations exceeded');
    OUTPUT $\boldsymbol{\sigma} = (\sigma_1, \ldots, \sigma_v)$.
    STOP.
Step 13 OUTPUT $\boldsymbol{\sigma} = (\sigma_1, \ldots, \sigma_{M_t})$.

We can observe that if an area of the square of the volatility function $\int_0^\tau \sigma^2(t)dt$ is the same, the option price is the same from the structure of the modified BS formula (10).

Therefore, we consider the post-processing of the piecewise-constant volatility function based on the structure of the BS formula. Let $N_0 = 0$, N_v be the number of time steps for the expiration date T_v, $v = 1, \ldots, M_t$ and let $W^n = V_{\boldsymbol{\sigma}}^2(n\Delta t)$. The piecewise volatility constants $\boldsymbol{\sigma} = (\sigma_1, \ldots, \sigma_{M_t})$ are given by Algorithm 1. We define the $Area_v$ for $v = 1, \ldots, M_t$ as

$$Area_v(W) = \left(\frac{W^{N_{v-1}}}{2} + \sum_{n=N_{v-1}+1}^{N_v-1} W^n + \frac{W^{N_v}}{2}\right)\Delta t,$$

and define the r_v for $v = 1, \ldots, M_t - 1$ as

$$r_v(W) = \frac{W^{N_v} + W^{N_v+1}}{2} - W^{N_v-1}.$$

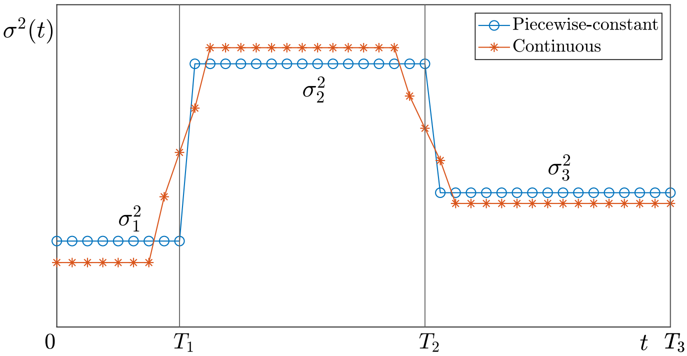

Fig. 2 Schematic of the proposed post-processing

Given a positive integer d, we define the following modified volatility function $\bar{W}^n$.

$$\bar{W}^n = \begin{cases} W^{N_v - 1} + r_v(W)(n - N_v + d), & \text{if } N_v - d + 1 \le n \le N_v + d - 1, \quad 1 \le v \le M_t - 1, \\ W^n, & \text{otherwise.} \end{cases}$$

Here, d is the parameter for the width of the transition layer and the number of node points on the transition layer becomes $(2d - 1)$. Thus, the larger d, the wider the width of the transition layer. We consider $\tilde{W}$ to equalize the $Area_v(W)$ and the $Area_v(\tilde{W})$ for $v = 1, \ldots, M_t$ as follows.

$$\tilde{W}^n = \begin{cases} \bar{W}^n + a_1, & \text{if } N_0 \le n \le N_1 - d, \\ \bar{W}^n + a_v, & \text{if } N_{v-1} + d \le n \le N_v - d, \quad 2 \le v \le M_t - 1, \\ \bar{W}^n, & \text{if } N_v - d + 1 \le n \le N_v + d - 1, \quad 1 \le v \le M_t - 1, \\ \bar{W}^n + a_{M_t}, & \text{if } N_{M_t - 1} + d \le n \le N_{M_t}, \end{cases}$$

where

$$a_v = \begin{cases} \dfrac{Area_v(W) - Area_v(\bar{W})}{\Delta t\,(N_1 - d + 1.5)}, & \text{if } v = 1, \\ \dfrac{Area_v(W) - Area_v(\bar{W})}{\Delta t\,(N_v - N_{v-1} - 2d + 1)}, & \text{if } 2 \le v \le M_t - 1, \\ \dfrac{Area_v(W) - Area_v(\bar{W})}{\Delta t\,\left(N_{M_t} - N_{M_t - 1} - d + 1.5\right)}, & \text{if } v = M_t. \end{cases}$$

Then, we define the post-piecewise volatility function as

$$\sigma^n = \sqrt{\tilde{W}^n}.$$

3 Computational tests

In this section, we perform computational tests using manufactured piecewise-constant volatility function and real financial market price data to validate the accuracy and robustness of the proposed reconstruction of time-dependent continuous volatility. The option quotes are generated using the modified BS formula (10) from the manufactured piecewise-constant volatility function.

Algorithm 2 Post-processing of piecewise-constant volatility function

INPUT piecewise volatility function $V_{\boldsymbol{\sigma}}(t)$; number N_v of time steps for the expiration date T_v for $v = 1, \ldots, M_t$; integer $d \geq 1$.
OUTPUT continuous volatility function $\sigma(n\Delta t)$ for $n = 1, \ldots, N_{M_t}$.
Step 1 Set $W^n = V_{\boldsymbol{\sigma}}^2(n\Delta t)$;
Step 2 For $v = 1, \ldots, M_t$ do Steps 3 and 4
  Step 3 Set $A_v = Area_v(W)$.
  Step 4 If $v \leq M_t - 1$ then set $\alpha_v = r_v(W)$.
Step 5 For $n = 1, \ldots, N_{M_t}$
  set $\bar{W}^n = W^n$.
Step 6 For $v = 1, \ldots, M_t - 1$
  for $n = N_v - d + 1, N_v - d + 2, \ldots, N_v + d - 1$
  set $\bar{W}^n = \alpha_v(n - N_v + d)$.
Step 7 For $v = 1, \ldots, M_t$ do Steps 8 and 9
  Step 8 Set $B_v = Area_v(\bar{W})$.
  Step 9 If $v = 1$ then set $a_v = (A_v - B_v)/(\Delta t(N_v - d + 1.5)$.
  else if $2 \leq v \leq M_t - 1$ then set $a_v = (A_v - B_v)/(\Delta t(N_v - N_{v-1} - 2d + 1)$.
  else set $a_v = (A_v - B_v)/(\Delta t(N_v - N_{v-1} - d + 1.5)$.
Step 10 For $n = 1, \ldots, N_{M_t}$
  set $\tilde{W}^n = \bar{W}^n$.
Step 11 For $n = 1, \ldots, N_1 - d$
  set $\tilde{W}^n = \bar{W}^n + a_1$.
Step 12 For $v = 2, \ldots, M_t - 1$
  for $n = N_{v-1} + d, N_{v-1} + d + 1, \ldots, N_v - d$
  set $\tilde{W}^n = \bar{W}^n + a_v$.
Step 13 For $n = N_{M_t-1} + d, N_{M_t-1} + d + 1, \ldots, N_{M_t}$
  set $\tilde{W}^n = \bar{W}^n + a_{M_t}$.
Step 14 OUTPUT $\sigma(n\Delta t) = \sqrt{\tilde{W}^n}$.

3.1 Manufactured data 1

Let a manufactured piecewise-constant volatility function be defined as

$$\sigma(t) = \begin{cases} 0,3, & 0 \leq t \leq T_1, \\ 0.6, & T_1 < t \leq T_2, \\ 0.3, & T_2 < t \leq T_3. \end{cases} \tag{11}$$

The reference values for the call option are derived from these manufactured volatility functions by solving Eq. (3) with $T = 360$ and $K_p = 70 + 10p$ for $p = 1, 2, \ldots, 5$. We use strike prices $K_p = 70 + 10p$ for $p = 1, 2, \ldots, 5$ and expiration dates $T_1 = 120\Delta\tau$, $T_2 = 240\Delta\tau$, and $T_3 = 360\Delta\tau$, where $\Delta\tau = 1/360$. The parameters used are $r = 0.1$, $S_0 = 100$, $\sigma_1 = 0.5$, $d = 10$, $N = 1500$, and $tol = 1.0e\text{-}16$. Tables 1 and 2 list the numerical prices calculated by the manufactured volatility and reconstructed continuous volatility, respectively.

Table 1 Option prices generated using the modified BS formula (10) from the volatility function (11)

K_p	80	90	100	110	120
$T_1 = 120\Delta\tau$	23.08	14.88	8.55	4.37	2.00
$T_2 = 240\Delta\tau$	29.48	23.37	18.30	14.17	10.86
$T_3 = 360\Delta\tau$	32.12	26.20	21.18	17.00	13.54

Table 2 Numerical prices generated by the reconstructed continuous volatility function

K_p	80	90	100	110	120
$T_1 = 120\Delta\tau$	23.06	14.89	8.56	4.36	1.93
$T_2 = 240\Delta\tau$	29.50	23.39	18.31	14.17	10.86
$T_3 = 360\Delta\tau$	32.21	26.24	21.18	16.97	13.49

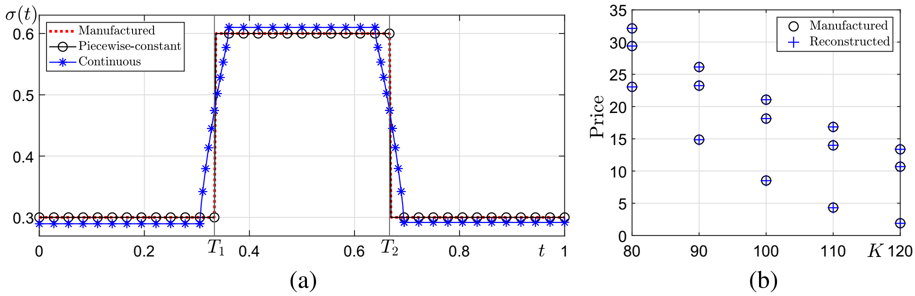

Fig. 3 (**a**) The manufactured volatility function and the reconstructed volatility function, (**b**) calculated prices

Figure 3 shows the manufactured volatility function, the reconstructed volatility function using the proposed algorithm, and the calculated prices by the BS equation.

3.2 Manufactured data 2

Let a manufactured continuous volatility function be defined as

$$\sigma(t) = -(t - 0.4)^2 + 0.05\sin(15\pi t) + 0.7. \tag{12}$$

The reference values for the call option are obtained based on these manufactured volatility functions by solving Eq. (3) with $T = 360$ and $K_p = 70 + 10p$ for $p = 1, 2, \ldots, 5$. We use strike prices $K_p = 70 + 10p$ for $p = 1, 2, \ldots, 5$ and expiration dates $T_1 = 120\Delta\tau$, $T_2 = 240\Delta\tau$, and $T_3 = 360\Delta\tau$, where $\Delta\tau = 1/360$. The parameters used are $r = 0.1$, $S_0 = 100$, $\sigma_1 = 0.5$, $d = 4$, $N = 1500$, and $tol = 1.0e\text{-}16$

Tables 3 and 4 list the numerical prices calculated by the manufactured volatility and reconstructed continuous volatility, respectively.

Figure 4 shows the manufactured volatility function, the reconstructed volatility function using the proposed algorithm with $d = 4$, and the calculated prices by the BS equation.

Next, we consider the effect of the post-processing parameter d. The post-processing parameter uses $d = 12,\ 36$ and the other parameters are the same as the above simulation. Table 5 lists the European call option prices calculated by the reconstructed volatility function with post-processing parameter $d = 12$.

Table 3 Option prices generated using the modified BS formula (10) from the volatility function (12)

K_p	80	90	100	110	120
$T_1 = 120\Delta\tau$	27.33	21.22	16.22	12.25	9.16
$T_2 = 240\Delta\tau$	33.62	28.40	23.94	20.14	16.93
$T_3 = 360\Delta\tau$	37.20	32.32	28.07	24.38	21.17

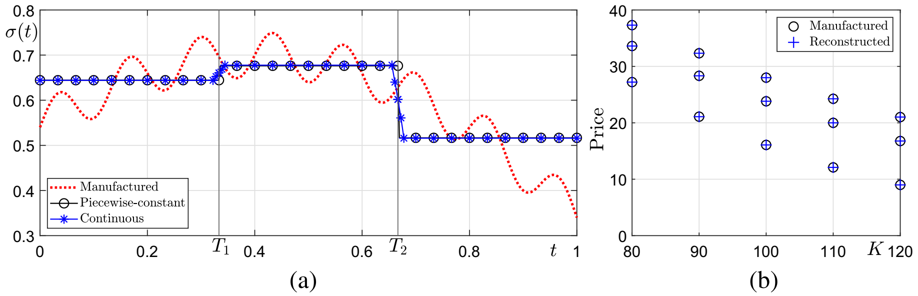

Fig. 4 (**a**) The manufactured volatility function and the reconstructed volatility function with $d = 4$, (**b**) calculated prices

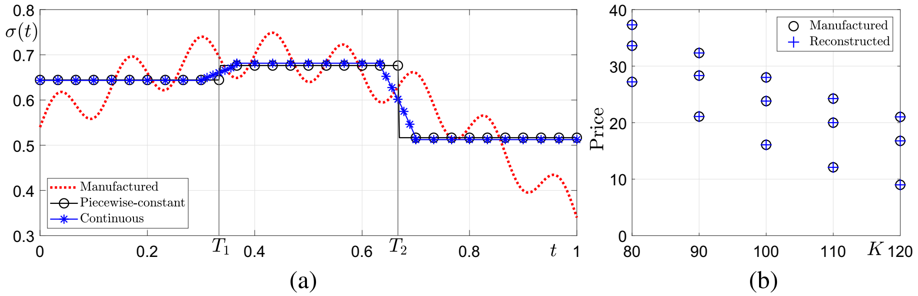

Fig. 5 (**a**) The manufactured volatility function and the reconstructed volatility function with $d = 12$, (**b**) calculated prices

Figure 5 shows the manufactured volatility function, the reconstructed volatility function with post-processing parameter $d = 12$ using the proposed algorithm, and the calculated prices by the BS equation.

Table 6 lists the European call option prices calculated by the reconstructed volatility function with post-processing parameter $d = 36$.

Figure 6 shows the manufactured volatility function, the reconstructed volatility function with post-processing parameter $d = 36$ using the proposed algorithm, and the calculated prices by the BS equation.

Table 4 Numerical prices generated by the reconstructed continuous volatility function with $d = 4$

K_p	80	90	100	110	120
$T_1 = 120\Delta\tau$	27.33	21.22	16.23	12.25	9.15
$T_2 = 240\Delta\tau$	33.70	28.43	23.93	20.11	16.89
$T_3 = 360\Delta\tau$	37.36	32.38	28.06	24.32	21.08

Table 5 Numercial prices generated by the reconstructed continuous volatility function with $d = 12$

K_p	80	90	100	110	120
$T_1 = 120\Delta\tau$	27.33	21.22	16.23	12.25	9.15
$T_2 = 240\Delta\tau$	33.70	28.43	23.93	20.11	16.89
$T_3 = 360\Delta\tau$	37.36	32.38	28.06	24.32	21.08

Table 6 Numerical prices generated by the reconstructed continuous volatility function with $d = 36$

K_p	80	90	100	110	120
$T_1 = 120\Delta\tau$	27.32	21.22	16.23	12.25	9.15
$T_2 = 240\Delta\tau$	33.70	28.43	23.93	20.11	16.89
$T_3 = 360\Delta\tau$	37.36	32.38	28.06	24.32	21.08

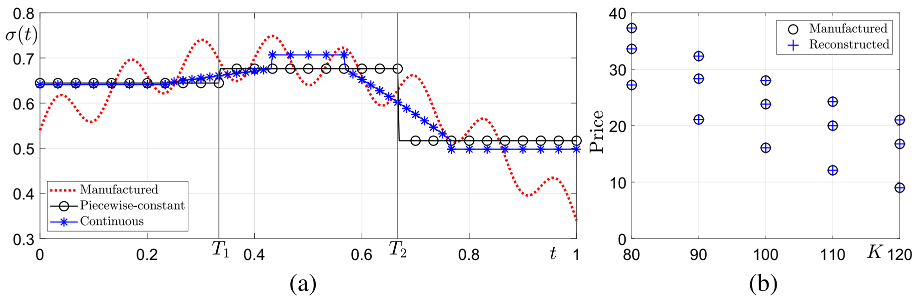

Fig. 6 (**a**) The manufactured volatility function and the reconstructed volatility function with $d = 36$, (**b**) calculated prices

Table 7 Premiums for KOSPI 200 index call options at different strikes and expiration dates on 15 January 2024

K_p	360.0	362.5	365.0	367.5	370.0	372.5	375.0
$T_1 = 24\Delta\tau$	0.59	0.43	0.32	0.23	0.17	0.12	0.09
$T_2 = 52\Delta\tau$	2.24	1.84	1.47	1.17	0.96	0.76	0.61
$T_3 = 87\Delta\tau$	3.12	2.82	2.21	2.00	1.60	1.29	1.16

We can observe that the calculated European call option prices for post-processing parameters $d = 4,\ 12,\ 36$ are the same, which means that there is no effect on the calculation of the option price. Numerical results show that if the area of the square of the volatility function by the post-processing is the same, the option price is the same by the structure of the BS formula (10).

3.3 KOSPI 200

In this subsection, we reconstruct the volatility function for the KOSPI 200 index call option using the proposed algorithm. The market data for the KOSPI 200 index call option on 15 January 2024 is provided by Korea Exchange (KRX Market Data System: https://data.krx.co.kr/). We use strike prices $K = 357.5 + 2.5p$ for $p = 1, \ldots, 7$ and expiration dates $T_1 = 24\Delta\tau$, $T_2 = 52\Delta\tau$, and $T_3 = 87\Delta\tau$. The parameters used are the 3-month certificate of deposit rate of Korea $r = 0.0381$, $S_0 = 339.24$, $\sigma_1 = 0.5$, $d = 10$, $N = 1500$, and $tol = 1.0e\text{-}16$ The premiums for KOSPI 200 index call options at different strikes and maturities are given in Table 7. Figure 7 shows the reconstructed volatility function using the proposed algorithm and the calculated prices by the BS equation for the KOSPI 200 index call option.

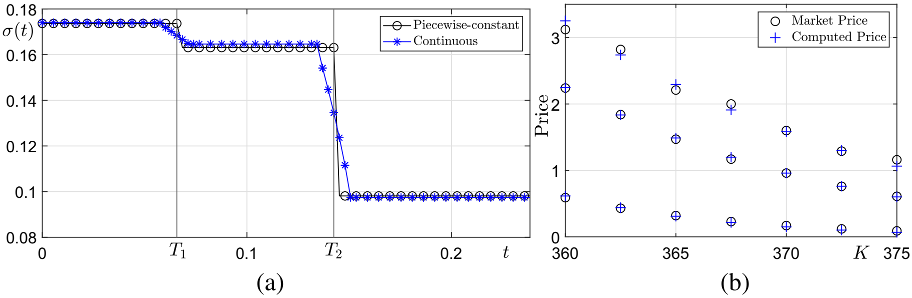

Fig. 7 (**a**) The manufactured volatility function and the reconstructed volatility function, (**b**) calculated prices

4 Conclusions

In this paper, we proposed a robust and accurate method for reconstructing the time-dependent continuous volatility function using observed option prices from the financial market and the BS equation. The proposed algorithm comprises two steps: First, the time-dependent piecewise-constant volatility function is calculated by the steepest descent method. Second, a continuous volatility function is reconstructed by continuously connecting the jumps of the piecewise-constant volatility values at the expiration dates. We performed computational tests using the manufactured volatility function and KOSPI 200 call option prices. The computational simulation results demonstrated that the proposed method can reconstruct continuous volatility functions accurately in a robust way. As future research work, we will extend the proposed methodology to reconstructing the local volatility surface (Kwak et al. 2022).

Acknowledgements The corresponding author (J.S. Kim) was supported by the Brain Korea 21 FOUR through the National Research Foundation of Korea funded by the Ministry of Education of Korea. The authors are grateful to the reviewers for constructive and helpful comments on the revision of this article.

Data availability Data are available from the corresponding author upon reasonable request.

Declarations

Conflict of interest All the authors declare that they have no Conflict of interest.

References

Ames WF (2014) Numerical methods for partial differential equations. Academic Press, New York

Black F, Scholes M (1973) The pricing of options and corporate liabilities. J Polit Econ 81(3):637–654. https://doi.org/10.1086/260062

Crépey S (2003) Calibration of the local volatility in a generalized Black-Scholes model using tikhonov regularization. SIAM J Math Anal 34(5):1183–1206. https://doi.org/10.1137/S0036141001400202

Gatheral J, Hsu EP, Laurence P, Ouyang C, Wang TH (2012) Asymptotics of implied volatility in local volatility models. Math Financ 22(4):591–620. https://doi.org/10.1111/j.1467-9965.2010.00472.x

Georgiev SG, Vulkov LG (2019) Computation of time-dependent implied volatility from point observations for European options under jump-diffusion models. AIP Conf Proc 2172:1. https://doi.org/10.1063/1.5133542

Georgiev SG, Vulkov LG (2020) Computational recovery of time-dependent volatility from integral observations in option pricing. J Comput Sci 39:101054. https://doi.org/10.1016/j.jocs.2019.101054

Georgiev SG, Vulkov LG (2021) Fast reconstruction of time-dependent market volatility for European options. Comput Appl Math 40(1):30. https://doi.org/10.1007/s40314-021-01422-9

Iqbal S, Wei Y (2021) Recovery of the time-dependent implied volatility of time fractional Black–Scholes equation using linearization technique. J Inverse Ill-Posed Probl 29(4):599–610. https://doi.org/10.1515/jiip-2020-0105
Itkin A, Lipton A (2018) Filling the gaps smoothly. J Comput Sci 24:195–208. https://doi.org/10.1016/j.jocs.2017.02.003
Jeong D, Yoo M, Kim J (2016) Accurate and efficient computations of the Greeks for options near expiry using the Black-Scholes equations. Discrete Dyn Nat Soc 2016:1586786. https://doi.org/10.1155/2016/1586786
Jiang L, Li C (2005) Mathematical modeling and methods of option pricing. World Scientific, Singapore
Jin Y, Wang J, Kim S, Heo Y, Yoo C, Kim Y, Kim J, Jeong D (2018) Reconstruction of the time-dependent volatility function using the Black–Scholes model. Discrete Dyn Nat Soc 2018:3093708. https://doi.org/10.1155/2018/3093708
Kim HG, Cho SY, Kim JH (2023) A martingale method for option pricing under a CEV-based fast-varying fractional stochastic volatility model. Comput Appl Math 42(6):296. https://doi.org/10.1007/s40314-023-02432-5
Kim S, Han H, Jang H, Jeong D, Lee C, Lee W, Kim J (2021) Reconstruction of the local volatility function using the Black–Scholes model. J Comput Sci 51:101341. https://doi.org/10.1016/j.jocs.2021.101341
Kwak S, Hwang Y, Choi Y, Wang J, Kim S, Kim J (2022) Reconstructing the local volatility surface from market option prices. Mathematics. https://doi.org/10.3390/math10142537
Lee C, Kwak S, Hwang Y, Kim J (2023) Accurate and efficient finite difference method for the Black–Scholes model with no far-field boundary conditions. Comput Econ 61(3):1207–1224. https://doi.org/10.1007/s10614-022-10242-w
Park E, Lyu J, Kim S, Lee C, Lee W, Choi Y, Kwak S, Yoo C, Hwang H, Kim J (2022) Calibration of the temporally varying volatility and interest rate functions. Int J Comput Math 99(5):1066–1079. https://doi.org/10.1080/00207160.2021.1948539
Rodrigo MR, Mamon RS (2006) An alternative approach to solving the Black-Scholes equation with time-varying parameters. Appl Math Lett 19(4):398–402. https://doi.org/10.1016/j.aml.2005.06.012
Schied A, Stadje M (2007) Robustness of delta hedging for path-dependent options in local volatility models. J Appl Probab 44(4):865–879. https://doi.org/10.1239/jap/1197908810
Windcliff H, Forsyth PA, Vetzal KR (2004) Analysis of the stability of the linear boundary condition for the Black-Scholes equation. J Comput Financ 8:65–92. https://doi.org/10.21314/JCF.2004.116
Wyns M, In't Hout KJ (2018) An adjoint method for the exact calibration of stochastic local volatility models. J Comput Sci 24:182–194. https://doi.org/10.1016/j.jocs.2017.02.004
Yoon Y, Seo JH, Kim JH (2022) Closed-form pricing formulas for variance swaps in the Heston model with stochastic long-run mean of variance. Comput Appl Math 41(6):235. https://doi.org/10.1007/s40314-022-01939-7
Zhang Q, Song H, Hao Y (2022) Semi-implicit FEM for the valuation of American options under the Heston model. Comput Appl Math 41(2):73. https://doi.org/10.1007/s40314-022-01764-y
Zhao JJ, Xu ZL (2022) Calibration of time-dependent volatility for European options under the fractional Vasicek model. AIMS Math 7:11053–11069. https://doi.org/10.3934/math.2022617